Journal of Materials Chemistry C

COMMUNICATION

View Article Online
View Journal | View Issue

Cite this: J. Mater. Chem. C, 2017, 5, 9534

Received 9th July 2017,
Accepted 6th September 2017

DOI: 10.1039/c7tc03043f

rsc.li/materials-c

Pristine graphene oxide film-based contactless actuators driven by electrostatic forces†

Yi He,[ab] Yajuan Sun,[c] Zhe Wang,[a] Shaoyang Ma,[a] Nan Zhang,[a] Jing Zhang,[a] Siowling Soh[c] and Lei Wei *[a]

Graphene oxide (GO)-based actuators provide a material-centered mechanism to enable a broad range of promising applications, especially in artificial muscles, sensors, switches, and energy harvesting devices. However, the current fabrication methods of such actuators require the complicated synthesis of GO-based composites that inevitably break the intrinsic structure of GO. Moreover, the obtained actuators are commonly driven by a strong external stimulus (light, moisture, or electricity) with unavoidable direct contact, which results in the decomposition of the GO-based composites, and thus reduces the device lifetime. To address the aforementioned challenges and limitations, we demonstrate a simple and generic electrostatic actuation principle for the design and fabrication of pristine GO film-based contactless actuators with a fast actuation response, good reversible actuation, and high stability. The resulting GO film-based actuators can be driven easily by almost all commonly charged objects. Two applications are demonstrated, one is a smart "radar" made by a 3 × 3 GO film strip array for tracking the motion of objects, and the other one is GO film-based "dancers" obtained from Chinese paper-cuts. The presented contactless actuation principle and the simple fabrication process open a new avenue for the design and development of GO-based actuators, which can be easily extended to the fabrication of other smart devices for motion detection or energy harvesting.

Actuators which transfer external stimuli to mechanical responses have enabled a broad range of promising applications, especially in artificial muscles, sensors, switches, and energy harvesting devices.[1] The performance of actuators has focused to date on the development of new materials.[2] Various materials, such as electroactive polymers, shape memory polymers, hydrogels, carbon nanotubes, and graphene (G) and its derivatives,[3] have been intensively employed for realizing a rich variety of actuators based on their responses to electric fields, humidity, or light. Among all the demonstrated materials, graphene oxide (GO) and GO-based nanocomposites are preferable for constructing actuators owing to their extraordinary properties including high thermal conductivity, light weight, good electrical properties and photo-thermal conversion.[4] For example, asymmetric G/GO fibers can respond to moisture, because GO has a stronger affinity to water than G, displaying well-controlled deformation and motion.[5] In addition, polydopamine-modified reduced GO/Norland Optical Adhesive-63 films are used for the demonstration of near-infrared (NIR) light driven-bilayer actuators based on the NIR absorption of reduced GO.[6] Very recently, partially reduced GO/polypyrrole composite films have been applied in moisture and electrochemical actuators.[7] However, these reported GO-based actuators are mainly based on composites which require multi-step and complicated synthesis procedures. During these procedures, the intrinsic structure of GO is inevitably broken. Moreover, these actuators require a strong external stimulus (light, moisture, or electricity), which essentially limits their applications. Furthermore, they require direct contact with external stimuli, which may decrease the device lifetime because light, moisture or electricity can result in the decomposition of GO-based composites.[8] Therefore, exploitation of pristine GO-based actuators with a contactless actuation mechanism remains fundamentally challenging.

Contact electrification is a common phenomenon in which material surfaces bear charges as a result of contact.[9] The charged object can be attracted or repelled by the electrostatic force in the presence of an electrostatic field. More importantly, the electrostatic field from contact electrification is everywhere, and almost all the materials such as metals, polymers, water and the human body bear different charges.[10] When a charged object is close to other charged objects, the electrostatic field between them changes, which leads to the motion of objects. Hence, the use of an electrostatic force to drive the motion of light-weight films is an ideal way to achieve contactless actuators.

Here we present a contactless actuator based on a pristine GO film fabricated by a simple solvent evaporation technique

[a] School of Electrical and Electronic Engineering, Nanyang Technological University, 50 Nanyang Avenue, 639798, Singapore. E-mail: wei.lei@ntu.edu.sg
[b] School of National Defence Science & Technology, Southwest University of Science and Technology, Mianyang 621010, P. R. China
[c] Department of Chemical and Biomolecular Engineering, National University of Singapore, 4 Engineering Drive, 117585, Singapore

† Electronic supplementary information (ESI) available. See DOI: 10.1039/c7tc03043f

and a commercially available plastic Petri dish. The resulting actuator is driven by an electrostatic actuation mechanism with a wide spectrum of charged objects, such as weighing paper, glass slides, metal tweezers, human fingers, and polytetrafluoroethene (PTFE) films. Additionally, the resulting actuator shows a large deflection and a fast response to a weak electrostatic field variation. Two applications are demonstrated to validate the resulting GO film. One is a smart "radar" made by a 3 × 3 GO film strip array for tracking the motion of objects, and the other one is GO film-based "dancers" obtained from Chinese paper-cuts. The present strategy provides an alternative methodology for the design and fabrication of high-performance actuators to address the aforementioned challenges, thus leading to promising applications in energy harvesting, sensing, and other related fields.

The GO film is prepared *via* a solvent evaporation technique. Fig. 1a shows the fabrication process of the GO film. 50 mL of 0.9 mg mL^{-1} GO suspension solution is poured into a glass Petri dish and evaporated at 50 °C for 24 hours. The GO film is obtained by directly peeling it off from the dish (see the material and synthesis of GO films in the method section). As shown in Fig. 1b, the optical image of GO indicates that the diameter of the obtained GO film is about 9.5 cm. Scanning electron microscope (SEM) and atomic force microscope (AFM) images demonstrate that some quasi-one-dimensional creases are observed in the obtained GO film (Fig. 1c and Fig. S1, ESI†). Fig. 1d exhibits the cross-selection SEM image of the obtained GO film, which clearly illustrates that the GO film with a thickness of about 4 μm has a multilayered structure, similar to that reported previously.[11] The crystal structure of the GO film is studied by X-ray diffraction (XRD), as shown in Fig. S2 (ESI†). The XRD peak of the obtained GO film is centered at $2\theta = 10.9^{\circ}$, suggesting that the layer distance between the sheets of the GO film is approximately 0.8 nm. Furthermore, Raman spectroscopy is employed to investigate the structure of the resulting GO film. As displayed in Fig. S3 (ESI†), two peaks at 1355 cm^{-1} and 1595 cm^{-1} are observed, which are ascribed to the D and G bands of GO, respectively. Fourier transform infrared (FTIR) spectroscopy is also performed to identify the surface composition of the obtained GO film. Fig. S4 (ESI†) shows the FTIR spectrum of the GO film. The typical peaks of the C=C stretching vibration appear at 1622 cm^{-1}, and for O–H deformation and stretching vibrations appear at 1400 cm^{-1} and 3385 cm^{-1}. The peaks at 1732 cm^{-1}, 1046 cm^{-1}, and 1220 cm^{-1} originate from the C=O stretching, alkoxy C–O stretching, and epoxy C–O vibration bands, respectively. These results identify that the GO film contains hydroxy, alkoxy, and epoxy groups.

To fabricate the GO film-based actuator, the resulting GO film is cut into strips with a length of 18.6 mm and a width of 2.0 mm. The obtained GO film strip is then attached onto the green sticker, and covered with a polystyrene (PS) Petri dish (diameter 8.6 cm, depth 1.8 cm) as shown in Fig. 2a. Because the PS dish bears a negative charge while the GO film strip bears a positive charge, the GO film strip is attracted and bends at a certain angle. In this bending state, the GO film strip becomes very sensitive to external charged objects and very weak attractive or repulsive forces may change the bending angle of the GO film strip, therefore resulting in the fast and reversible actuation of the GO film strip. As displayed in Fig. 2b, the bending angle increases as the negatively charged PTFE film moves closer to the GO film strip. And it goes back to the original state when the PTFE film is taken away. Inversely, a positively charged glass slide repels the GO film strip and decreases its bending angle when getting close to the GO film strip (Fig. 2c). The relationship between the distance and the bending angle of the GO film strip is studied based on the recorded videos (Movies 1 and 2, ESI†). Here the distance is defined as the vertical distance between the bottom of the charged object and the upper surface of the PS dish. As shown in Fig. 2d, both a negatively charged object and a positively charged object can controllably and reversibly drive the GO film

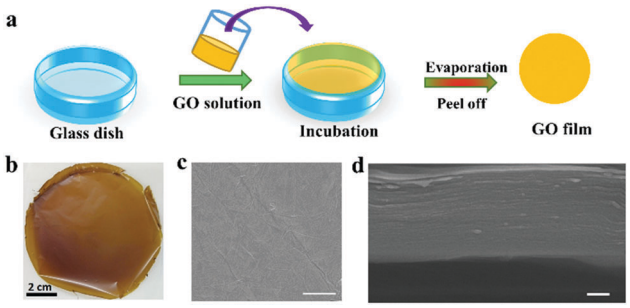

Fig. 1 (a) Schematic illustration of the fabrication process of GO films. (b) Optical image of the resulting GO film with a diameter of 9.5 cm. (c and d) SEM and cross-section SEM images of the resulting GO film (scale bar, 1 μm).

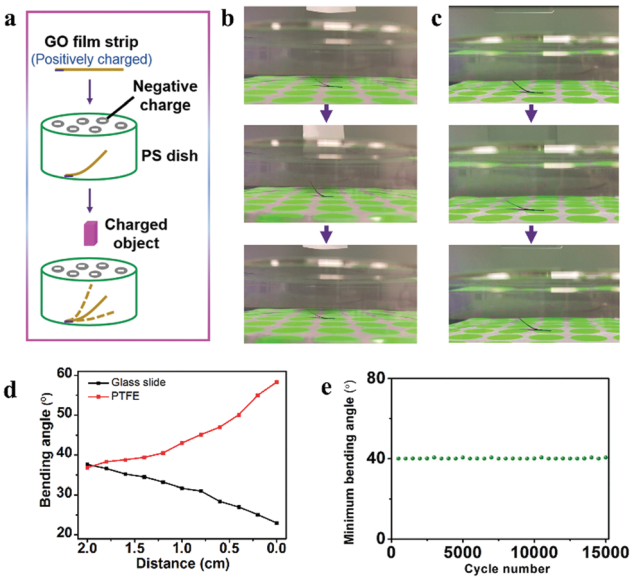

Fig. 2 (a) Schematic illustration of the GO film-based actuator. (b and c) Optical images showing the actuation process of a GO film strip driven by a PTFE film and a glass slide. (d) Bending angle as a function of the distance between the bottom of the charged object and the upper surface of the PS dish. (e) Dependence of the minimum bending angle on the cycle number.

strip based actuator. Moreover, the GO film strip based actuator exhibits a fast actuation speed in response to the movement of human fingers with reference to the changed area on the green sticker as shown in Movie 3 (ESI†). When a human finger approaches the surface of the dish, the GO film strip quickly bends at 39.5° within 0.56 s, and returns to its initial state in 0.75 s after the human finger moves away from the surface of the PS dish. A video camera is used to monitor the dynamic process of the actuator, and the corresponding bending angle can therefore be obtained and plotted as a function of time (Fig. S5, ESI†). The bending angle decreases when the human finger is close to the dish, and increases when it moves away. Besides, the performance reliability of the obtained actuator is evaluated. After being kept in a clean atmosphere for more than two months and then measured, the developed actuator still works well. Furthermore, we conduct the reliability test by fixing a metal tweezer on a linear motor. The reciprocating motion of the linear motor drives the positively charged tweezer to move close to and away from the GO film strip repeatedly. The GO film strip is repelled to its minimum bending angle when the tweezer moves close to the strip, and goes back to its original state as the tweezer moves away from it. The frequency of the reciprocating motion is 1.25 Hz, and we measure a minimum bending angle every 10 minutes. This test lasts for more than 200 minutes and the results show that the performance exhibits no evident change after 15 000 cycles (Fig. 2e), demonstrating its good reliability and stability.

More significantly, almost all commonly charged objects can easily drive the GO film-based actuator. Various objects including but not limited to gloves, weighing paper, and metal tweezers can cause the motion of the GO film-based actuator (Fig. S6–S8 and Movies 4–6, ESI†). As a result, the resulting actuator exhibits different response times and bending angles in response to different objects. Weighing paper, glass slides, and metal tweezers can lead to further bending of the actuator (repulsion force), while a PTFE film results in further attraction of the GO film, producing a larger bending angle than that of its initial state. These results indicate that the GO film actuator is generic, simple, and facile without the need for strong external stimuli.

The production, transportation, and use of the aforementioned objects produce static electricity. Accordingly, the driving force may be from the electrostatic force among the PS dish, various objects, and GO film. The triboelectric series of common materials are listed in Fig. S9 (ESI†). Human skin, glass, paper and steel are found to be located at the top of the triboelectric series, while PS and PTFE rank at the bottom. Therefore, PS and PTFE are apt at bearing negative charges, whereas human fingers, glass, weighing paper and metal tweezers (steel) tend to bear positive charges. The types of electric charge are experimentally identified by a Faraday cup connected to a high precision electrometer (Keithley 6514). The charge of the GO film is also tested, and the GO film bears positive charges with a surface charge density of about 0.5 μC m^{-2}. To investigate the origin of the surface charge, the GO film and reference materials are first discharged by using a Zerostat gun. After that, we contact the GO film 40 times with three reference materials (glass, paper, and PTFE). With an increase in the number of touches, the positive charge of the GO film increases (Fig. S10–S13, ESI†). Accordingly, the positive charge of the GO film mainly originates from contact electrification during the peeling process from a glass dish. When the GO film is reduced by hydroiodic acid, the reduced GO film also bears a similar positive charge, indicating that the charge of GO is not related to its surface groups. Therefore, the GO film strip bends when a charged object approaches due to the electrostatic force (Fig. S14a, ESI†).

To understand the mechanism of the actuator, the effect of humidity is firstly investigated. When the actuator is placed in a glove box without humidity, it can also be easily driven by a finger covered with a humidity-free glove (Movie 7, ESI†). This result eliminates the possibility of the humidity-induced deformation of the GO film strip. Subsequently, the interaction between the GO film strip and the PS dish is also studied. When the negatively charged PS dish is close to the GO film strip, it bends quickly (Fig. S14b and c, ESI†), indicating the presence of an attraction force between them. Additionally, the effect of different types of charge on bending of the GO film strip is studied. After a washcloth touches a glass rod, the washcloth acquires negative charges, and the glass rod acquires equal positive charges (Fig. S14d and e, ESI†). Evidently, the washcloth attracts the GO film strip, while the glass rod repels the GO film strip. The results demonstrate that the interaction between the GO film strip and the PS dish originates from electrostatic force. Since the electrostatic force is determined by an electrical field, the relationship between the electrical field and bending angles is studied to further clarify the mechanism. Fig. 3a and b show the set-up of this experiment. The PS dish is discharged by using a Zerostat gun to remove the influence of its surface charge. Then, the system is placed in a uniform

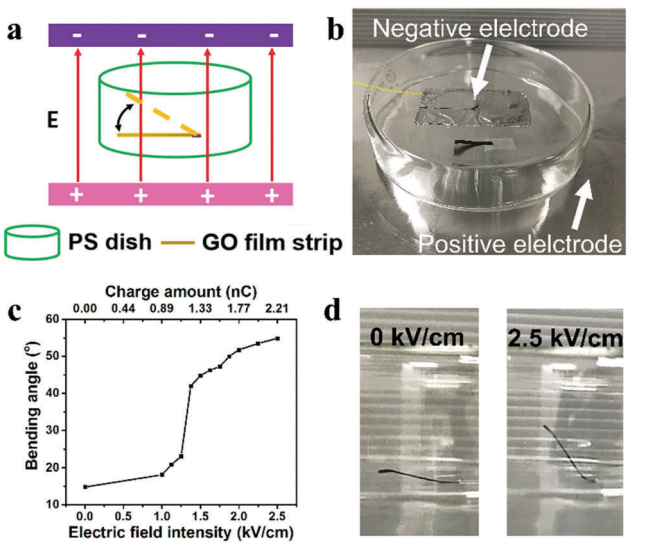

Fig. 3 (a) Schematic illustration and (b) optical image of GO film strip-based actuators driven by a uniform electrostatic field. (c) Bending angle as a function of the electric field intensity and the corresponding charge amount on the upper electrode. (d) Optical image showing the actuation process of a GO film strip driven by an electrostatic field.

electrostatic field which is generated by applying a direct voltage between two electrodes. The lower electrode is connected to the positive end and the upper electrode is connected to the negative end. As shown in Fig. 3c and Movie 8 (ESI†), with an increase in uniform electric field from 0 to 2.5 kV cm^{-1}, the bending angle of the GO film strip spans from 14.8° to 54.9°. Also, the charge amount on the upper electrode is calculated (electrode area: 10 cm^2), indicating that this actuator can be driven by less than 1 nC. Optical images in Fig. 3d intuitively show that the bending angle can be greatly changed below 2.5 kV cm^{-1}, corresponding to 2.21 nC. Accordingly, the inherent surface charge of GO is responsible for its bending. Thus, a GO film strip covered with a PS dish is attracted by an electrostatic force and finally bends at a certain angle to reach an equilibrium state. When the charged objects are placed on the surface of the PS dish, the electrostatic field changes and therefore breaks the equilibrium state, which results in a mechanical response of the GO film strip with the motion of charged objects. As a result, positively charged objects, such as human fingers, weighing paper, glass slides, and metal tweezers, cause further bending of the GO film strip because they repel the GO film strip. In contrast, negatively charged objects, such as a PTFE film, increase the negative charges of the PS dish area, which leads to less bending of the GO film strip as they attract the GO film strip.

In addition, an order-of-magnitude analysis electrostatic attractive force (FE) is carried out with the consideration of three models involving the GO film strip and the PS dish without the PTFE film, with the PTFE film at 5 cm (the distance between the surface of the PS dish and the PTFE film), and with the PTFE film at 1.5 cm as shown in Fig. S15 (ESI†), respectively. Using COMSOL Multiphysics, the FE in the case without the piece of PTFE film is calculated to be approximately 9.36 μN, which is slightly smaller than the weight of the GO film (4 mg in our case), since a force of around 9.8 μN can represent a weight of 1 mg. The reason is that this is only an order of magnitude analysis (1 mg is at the same order of magnitude as 4 mg), and we are thus only lifting one side of the GO film strip rather than lifting the whole GO film strip. Similarly, the electric potentials of the PS dish in the presence of the PTFE film at 5 cm and 1.5 cm are also solved, and the corresponding electrostatic attractive force is obtained to be 10.6 μN and 15.5 μN, respectively. The increase of the electrostatic attractive force FE between the GO film strip and the PS dish in the presence of the PTFE film results in less bending of the GO film strip, which is in good agreement with the observed experimental results. Furthermore, we also estimate the drag force accommodated by the actuator according to the drag equation in fluid dynamics: $F_D = 1/2C_D A\rho v^2$, where ρ is the air density, v is the relative speed between the GO film strip and air, C_D is the drag coefficient equal to 1.8 in our case,[12] and A is the area of the GO film strip. As a result, the drag force accommodated by the actuator is estimated to be 0.43 μN assuming that the GO film strip bends at a line speed of 10 cm s^{-1}.

The unique properties of GO film-based actuators driven by electrostatic forces mean that they can be used as a component for the development of various devices for practical applications

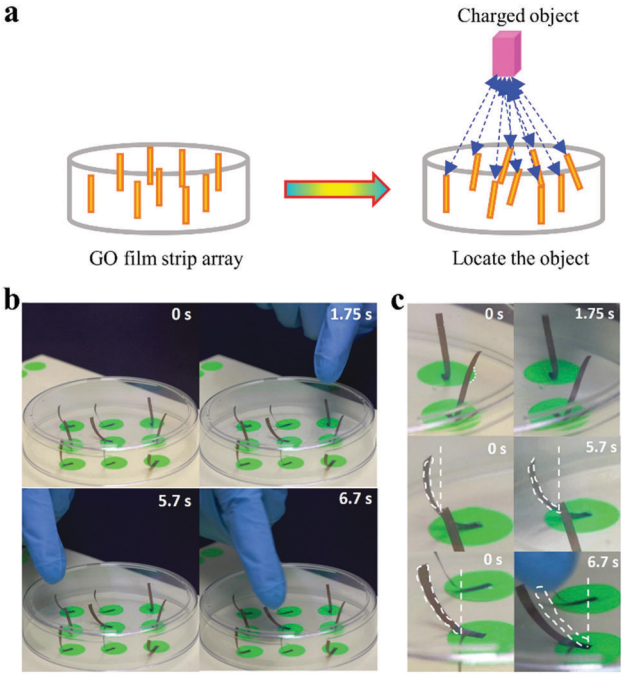

Fig. 4 (a) Schematic illustration of the design of a GO film array-based radar. (b) Optical images of the selective bending of the GO film array in response to a human finger covered with a glove at different positions. (c) Locally magnified images of the selective bending of the GO film array.

related to the motion of objects. For instance, the GO film-based actuators can be employed as a smart "radar" to identify the position of various objects. As shown in Fig. 4a, a radar is fabricated by a 3 × 3 GO film strip array with a grid size of 1.9 cm. When an object reaches above the surface of the PS dish, the GO film strips bend due to the electrostatic force. The GO film strips at different positions have different bending degrees which are proportional to the distance between the charged object and the GO film strip, thus locating various objects. Consider the motion of a human finger for example, the human finger located at different areas leads to the bending of the GO film strip (Fig. 4b, c and Movie 9, ESI†), in which the GO film strip close to the finger significantly bends. When the position of the finger changes, the GO film strip with the maximum bending degree changes accordingly. Hence, we can obtain the position information according to the bending degree of the GO film. This device may be potentially useful for next-generation electronic devices with contactless positioning interfaces.[13]

We further develop GO film-based dancers obtained by Chinese paper-cuts as another application demonstration. The dancer (width 1.6 cm and height 2.8 cm) is made by cutting a GO film into a human image and immobilizing it on the surface of the sticker with the help of glue. Three GO dancers are covered with the same PS dishes. As illustrated in Fig. 5, the GO dancers initially remain standing due to the attraction of the dish. When the finger arrives at the surface of the dish, the GO dancer instantly bends (Fig. 5a, b and Movie 10, ESI†), and will keep standing again as the finger moves away from the dish. Moreover, different fingers such as the index finger,

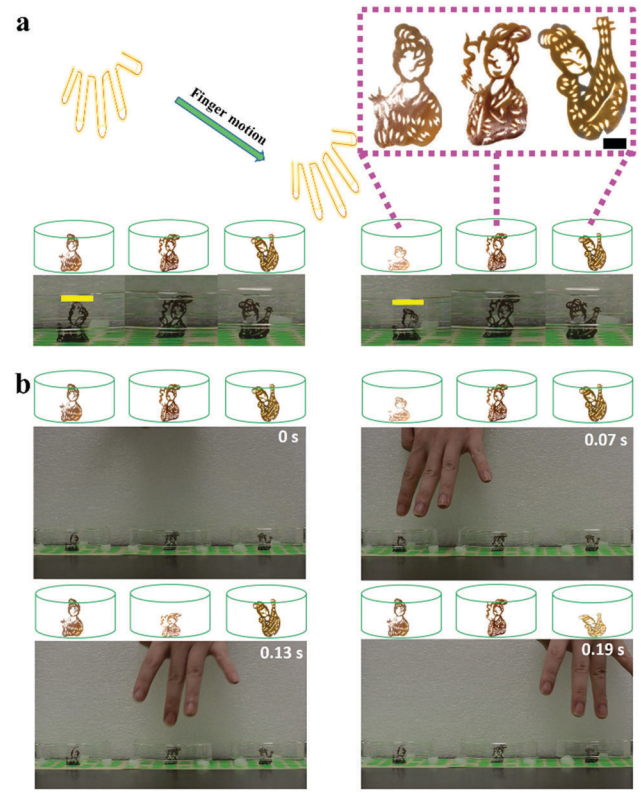

Fig. 5 (a) Schematic of GO film-based dancers and the corresponding images (scale bar, 0.5 cm). (b) Optical images of the motion of the GO film with the motion of human fingers, which can mimic the dancing process.

middle finger, and ring finger can individually cause the bending of the corresponding GO film dancer. When the fingers periodically arrive and leave from the surface of the dish, the GO dancer also periodically bends, leading to the dancing process. Consequently, the GO film-based dancer can sense the weak sound from the periodical bending of human fingers and provide a corresponding response. The GO film-based dancer also exhibits a good cyclic lifetime, and the deformation remains the same after 1000 cycles of actuation tests.

Conclusions

Traditionally, the GO film-based actuators require the preparation of various composites according to the processing steps, which are not compatible with conventional batch microfabrication steps. In our design, the GO film is directly prepared by a simple solvent evaporation technique. This simple synthetic approach allows for the preparation of GO films with different sizes and morphologies using different molds, which can be used for ultralow-power microchips and microdevices. The outstanding capacity of the GO film actuator for sensing the motion of human fingers can monitor human movement for the prevention of sports injury or the early diagnosis of Parkinson's disease. Besides, the GO film-based actuators can be further concatenated with other functional materials, for example, piezoelectric material polyvinylidene fluoride, leading to the realization of multi-functional flexible devices.

In summary, we propose a simple and generic electrostatic actuation principle for the design and fabrication of pristine GO film-based contactless actuators. Significantly, the fabrication process retains the inherent structure of the GO film. The developed contactless actuators show a fast actuation response, good reversible actuation, and high stability. Unlike the reported GO-based actuators that require strong external stimuli, the resulting GO film-based actuators can be driven easily by almost all commonly charged objects, demonstrating their generality and simplicity. More importantly, the actuators can be further used for practical applications, and smart radars and dancers are successfully fabricated and demonstrated for the first time. The present actuation principle opens a new avenue for the design and development of GO-based actuators, which can be easily extended to the fabrication of other smart devices for human motion monitors and energy harvesting *via* various rational designs.

Conflicts of interest

There are no conflicts to declare.

Acknowledgements

This work was supported in part by the Singapore Ministry of Education Academic Research Fund Tier 2 (MOE2015-T2-1-066 and MOE2015-T2-2-010), the Singapore Ministry of Education Academic Research Fund Tier 1 (RG85/16), and Nanyang Technological University (Start-up grant M4081515: Lei Wei). This work was also financially supported by the Singapore Ministry of Education under grant R-279-000-408-112.

Notes and references

1 (*a*) G. A. Salvatore, N. Münzenrieder, T. Kinkeldei, L. Petti, C. Zysset, I. Strebel, L. Büthe and G. Tröster, *Nat. Commun.*, 2014, **6**, 7258; (*b*) P. Chen, Y. Xu, S. He, X. Sun, S. Pan, J. Deng, D. Chen and H. Peng, *Nat. Nanotechnol.*, 2015, **10**, 1077–1083; (*c*) X. Zhang, Z. Yu, C. Wang, D. Zarrouk, J.-W. T. Seo, J. C. Cheng, A. D. Buchan, K. Takei, Y. Zhao and J. W. Agew, *Nat. Commun.*, 2014, **5**, 2983.

2 S. Park, J. An, J. W. Suk and R. S. Ruoff, *Small*, 2010, **6**, 210.

3 (*a*) Q. Zhao, J. W. Dunlop, X. Qiu, F. Huang, Z. Zhang, J. Heyda, J. Dzubiella, M. Antonietti and J. Yuan, *Nat. Commun.*, 2014, **5**, 4293; (*b*) O. Kim, T. J. Shin and M. J. Park, *Nat. Commun.*, 2013, **4**, 2208; (*c*) B. P. Lee and S. Konst, *Adv. Mater.*, 2014, **26**, 3415; (*d*) E. Wang, M. S. Desai and S.-W. Lee, *Nano Lett.*, 2013, **13**, 2826; (*e*) L. Kong and W. Chen, *Adv. Mater.*, 2014, **26**, 1025; (*f*) J. Mu, C. Hou, H. Wang, Y. Li, Q. Zhang and M. Zhu, *Sci. Adv.*, 2015, **1**, e1500533; (*g*) M. Ma, L. Guo, D. G. Anderson and R. Langer, *Science*, 2013, **339**, 186.

4 Y. Huang, J. Liang and Y. Chen, *J. Mater. Chem.*, 2012, **22**, 3671.

5 H. Cheng, J. Liu, Y. Zhao, C. Hu, Z. Zhang, N. Chen, L. Jiang and L. Qu, *Angew. Chem., Int. Ed.*, 2013, **52**, 10482.

6 M. Ji, N. Jiang, J. Chang and J. Sun, *Adv. Funct. Mater.*, 2014, **24**, 5412.
7 Y. Jiang, C. Hu, H. Cheng, C. Li, T. Xu, Y. Zhao, H. Shao and L. Qu, *ACS Nano*, 2016, **10**, 4735.
8 A. Hunt, D. A. Dikin, E. Z. Kurmaev, T. D. Boyko, P. Bazylewski, G. S. Chang and A. Moewes, *Adv. Funct. Mater.*, 2012, **22**, 3950.
9 J. Gunn, *Solid-State Electron.*, 1964, **7**, 739.
10 (*a*) L. S. McCarty and G. M. Whitesides, *Angew. Chem., Int. Ed.*, 2008, **47**, 2188; (*b*) B. Baytekin, H. T. Baytekin and B. A. Grzybowski, *J. Am. Chem. Soc.*, 2012, **134**, 7223; (*c*) X. Zhang, X. Huang, S. W. Kwok and S. Soh, *Adv. Mater.*, 2016, **28**, 3024; (*d*) H. Baytekin, A. Patashinski, M. Branicki, B. Baytekin, S. Soh and B. A. Grzybowski, *Science*, 2011, **333**, 308.
11 W. Guo, J. Chen, S. Sun and Q. Zhou, *J. Phys. Chem. C*, 2016, **120**, 7451.
12 A. Roshko, *NACA TN 3169*, 1954.
13 K. Szendrei, P. Ganter, O. Sànchez-Sobrado, R. Eger, A. Kuhn and B. V. Lotsch, *Adv. Mater.*, 2015, **27**, 6341.